PIONS IN HADRON PHYSICS*

J. Haidenbauer, W. Schäfer and J. Speth

Institut für Kernphysik, Forschungszentrum Jülich GmbH
52425 Jülich, Germany

(Received July 13, 2000)

The Jülich model for pion production in nucleon–nucleon collisions is reviewed. First calculations for recently measured spin correlation coefficients are presented. The influence of resonant [via the excitation of the $\Delta(1232)$] and nonresonant p-wave pion production mechanisms on these observables is examined. In the second part of the talk we discuss the role of pions in the $\bar{d}-\bar{u}$-asymmetry of the nucleon sea and its connection with the inclusive production of forward neutrons. We compare predictions for the pion structure function at small x with the data extracted from deep inelastic forward neutron production.

PACS numbers: 14.40.–n, 14.40.Aq

1. Introduction

The pion plays an outstanding role in nuclear and hadronic physics. It has an exceptional status in hadron physics because it is by far the lightest of all mesons, and its low mass, nearly one order of magnitude smaller than the typical hadronic mass scale, is connected with the chiral symmetry of QCD. In this respect it is also connected with the Partial Conservation of the Axial Current (PCAC). Due to its low mass it is also the mediator of the long range part of the nuclear force and it is therefore an important part of the nuclear many-body problem.

In the following we will discuss two extreme cases: we first review the theoretical status of pion production in proton–proton collisions near the pion threshold and second we discuss the importance of pions in inclusive and exclusive deep-inelastic electron scattering. We will show that the physics studied at the cooler synchrotrons at Jülich, Bloomington, and Uppsala is directly relevant to high-energy experiments at DESY, CERN, and Fermilab.

* Presented at the Meson 2000, Sixth International Workshop on Production, Properties and Interaction of Mesons, Cracow, Poland, May 19–23, 2000.

2. Pion production in *pp* scattering at threshold

Over the last few years the Jülich group has developed a meson-exchange model for the reaction $NN \to NN\pi$ near threshold [1,2] . In this model all standard pion-production mechanisms (direct production (Fig. 1(a)), pion rescattering (Fig. 1(b)) and contributions from pair diagrams (Fig. 1(c))) are considered. In addition, production mechanisms involving the excitation of the $\Delta(1232)$ resonance (*cf.* Fig. 1(d),(e)) are explicitly taken into account. All NN partial waves up to orbital angular momentum $L_{NN} = 2$, and all states with relative orbital angular momentum $l \leq 2$ between the NN system and the pion in the final state are considered. Furthermore all πN partial waves up to orbital angular momenta $L_{\pi N} = 1$ are included in calculating the rescattering diagrams of Fig. 1(b),(e). Thus, our model includes not only s-wave pion rescattering but also contributions from p-wave rescattering. The reaction $NN \to NN\pi$ is treated in a distorted wave Born approximation in the standard fashion. The actual calculations are carried out in momentum space. For distortions of the initial and final NN states we employ a variant of the full Bonn model [3] which explicitly includes the coupling to the $N\Delta$ as well as $\Delta\Delta$ channels. Thus the $NN \leftrightarrow N\Delta$ transition amplitudes and the NN T-matrices that enter in the evaluation of the pion production diagrams in Fig. 1 are consistent solutions of the same (coupled-channel) Lippmann–Schwinger-like equation. The $\pi N \to \pi N$ T-matrix needed for the rescattering process is likewise taken from a microscopic meson-exchange model developed by the Jülich group [4].

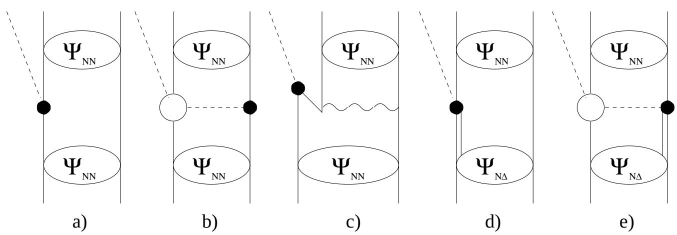

Fig. 1. Pion production mechanisms taken into account in our model: (a) direct production; (b) pion rescattering; (c) contributions from pair diagrams; (d) and (e) production involving the excitation of the $\Delta(1232)$ resonance. Note that diagrams where the Δ is excited after pion emission are also included.

Note that the pair diagrams (Fig. 1(c)) are viewed as an effective parametrization of contributions from additional short-range production mechanisms that are not yet fully understood, and are therefore not explicitly included in the model. Their strength, the only free parameter in the Jülich model, was adjusted to reproduce the total $pp\pi^0$ production cross section at low energies. Due to their vertex structure, these pair diagrams contribute only to s-wave pion production. Furthermore, they have practically no influence on the reactions $pp \to pn\pi^+$ and $pp \to d\pi^+$ [1].

Results for the total cross sections in all experimentally accessible channels are shown in Fig. 2 as a function of η, the maximum momentum of the produced pions in units of the pion mass. Evidently, the predictions of the model are in good overall agreement with the data over a wide energy range. We emphasize that the results for the channels $pp \to pn\pi^+$ and $pp \to d\pi^+$ do not involve any adjustable parameters, and are therefore genuine predictions of the model. Results for the production cross sections without inclusion of the Δ isobar are indicated in Fig. 2 by the dashed lines. These curves are obtained by setting the $\pi N\Delta$ coupling in the production operator equal to zero. Not surprisingly, for all reaction channels considered (except $pn \to pp\pi^-$) the Δ contributions play an important role at larger energies. One can also see however that they influence the cross section significantly even at energies near threshold.

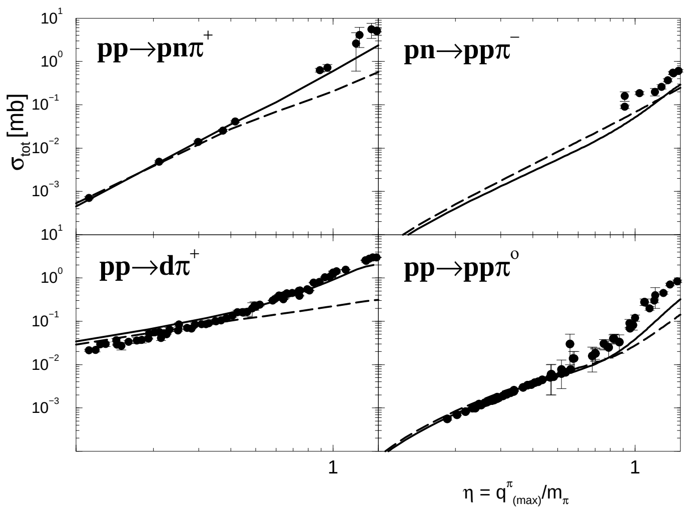

Fig. 2. Total cross section for $NN \to NN\pi$ in the different charge channels. The solid line shows the results for the full model. The dashed curve is the result without contributions involving the Δ (1232) excitation.

Our model is also in good quantitative agreement with other experimental information on pion production near threshold such as differential cross sections [5] and analyzing powers [1].

Very recently the first results from measurements of spin-dependent cross sections and spin correlation coefficients have been reported [6–9]. Such data are of great importance because it is expected that they might play an important role in improving our theoretical understanding of pion production near threshold. Here we will present the corresponding predictions of the Jülich model, and compare them with these new data. We will also investigate the sensitivity of these observables to specific production mechanisms.

Our results for the spin correlation coefficient combinations $A_\Sigma = A_{xx} + A_{yy}$, $A_\Delta = A_{xx} - A_{yy}$ and A_{zz} are shown in Fig. 3 for $pp \to pn\pi^+$ (left panel), $pp \to pp\pi^0$ (right panel), and $pp \to d\pi^+$ (middle panel). Data on the polar integrals of these observables are available for the first two processes [6, 8], while for $pp \to d\pi^+$ the angular dependence at $T_{\rm lab} = 400$ MeV ($\eta = 0.89$) has been measured [9]. (Note that the polar integrals of $-(A_{xx} + A_{yy})$ and A_{zz} yield the spin-dependent total cross section $\Delta\sigma_{\rm T}/\sigma_{\rm tot}$ and $\Delta\sigma_{\rm L}/\sigma_{\rm tot}$, respectively; *cf.* Refs. [6, 10] for definitions.)

One of the specific features of the Jülich model is that contributions from p-wave pion rescattering are fully taken into account. Their resonant part is given by pion production from the Δ excitation, as shown in Fig. 1(d). However our model also includes non-resonant contributions from p-wave pion rescattering. Thus we can study the influence of the latter on the spin observables [2]. Results in which the contributions of non-resonant p-wave pion rescattering were omitted are shown as dash-dotted curves in Fig. 3. One can see that the spin correlation coefficient combinations are significantly modified by the contributions from non-resonant p-wave rescattering, especially at higher energies.

The dashed curves in Fig. 3 show the effect of removing pion production via Δ excitation as well. Evidently this leads to rather large changes, which shows the important role the Δ plays in these spin-correlation parameters. Thus, these observables are very well suited for testing the model treatment of the pion-production contributions involving the Δ resonance. In particular, they allow one to examine the Δ contributions at energies far below the resonance regime. As can be seen from Fig. 3, the Δ has important effects at relatively low energies, especially in the reaction $pp \to pp\pi^0$.

Clearly, the predictions of our model are in excellent agreement with the data on the reactions $pp \to pn\pi^+$ and $pp \to d\pi^+$. It is interesting that contributions from pion-production from the Δ resonance as well as from (non-resonant) p-wave rescattering are required to achieve this agreement. With the Δ resonance alone (*cf.* the dash-dotted curves) the result would lie well below the experiment.

In the reaction $pp \to pp\pi^0$, however, only two of the measured observables are reasonably well reproduced by our model calculation, while A_Δ is overestimated by about a factor 2 (*cf.* Fig. 3). Since the result without non-resonant p-wave πN rescattering (dash-dotted curve) is close to the data one might be tempted to conclude that their contributions are overestimated in our model, as we argued in Ref. [1]. However, one should note that for energies corresponding to $\eta \approx 1$ our model underestimates the total π^0 pro-

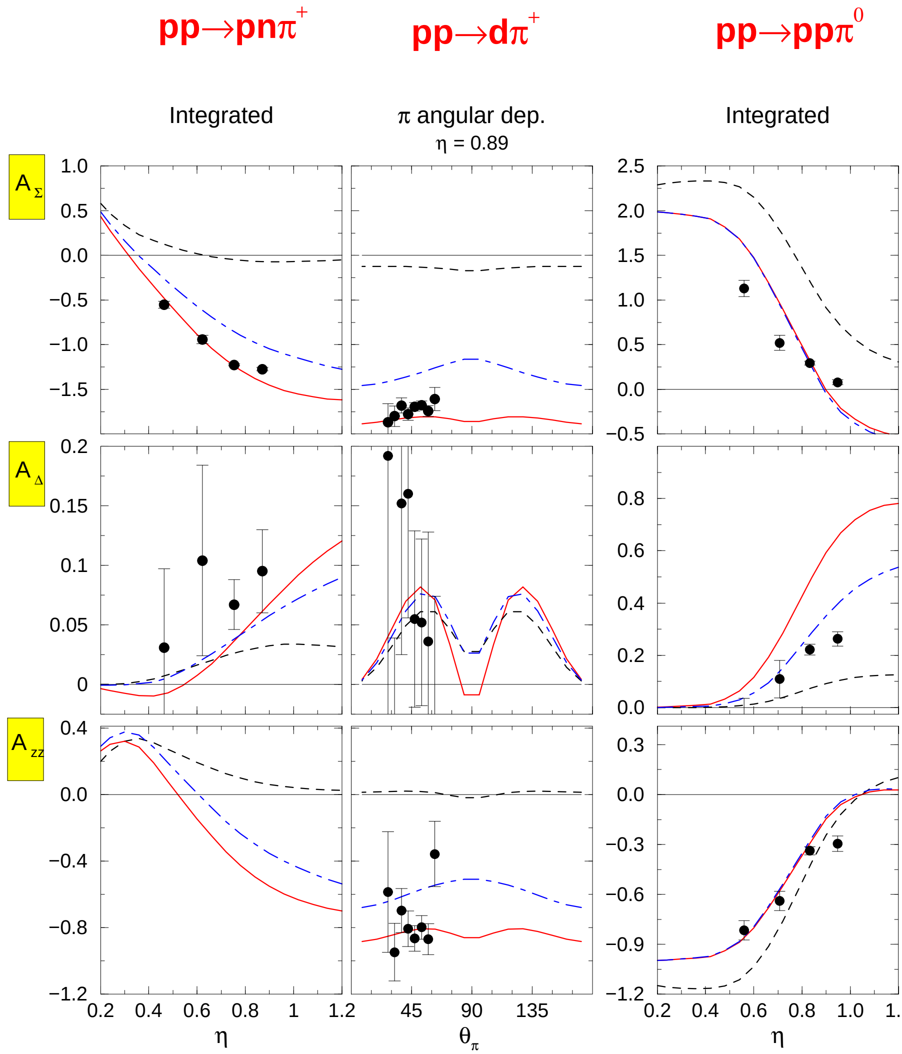

Fig. 3. Spin correlation parameters for the reactions $pp \to pn\pi^+$ (left panel), $pp \to d\pi^+$ (middle panel), and $pp \to pp\pi^0$ (right panel). $A_\Sigma = A_{xx} + A_{yy}$ and $A_\Delta = A_{xx} - A_{yy}$. The solid line represents the result of our full model. The dashed-dotted curves are obtained when the contributions of non-resonant p-wave pion rescattering are omitted. The dashed curves show results in which the contributions of the $\Delta(1232)$ resonance are also removed.

duction cross section already by about a factor of 2 (*cf.* Fig. 2). Since the spin correlation coefficients are normalized by $\sigma_{\rm tot}$ the disagreement with the data for A_Δ may simply reflect this discrepancy in the total cross section.

In any case, the reaction $pp \to pp\pi^0$ is much more sensitive to short-range production mechanisms than the other two channels. And obviously, those production processes are not yet properly described in our model.

3. Pions and the flavor structure of the nucleon sea

The phenomena discussed thus far have demonstrated the importance of treating the nonperturbative proton structure in terms of hadronic degrees of freedom. While the importance of pions in the nonperturbative structure of the proton, as probed in low and intermediate energy nuclear physics, is widely accepted, their role in high energy phenomena is often overlooked. An example that nicely demonstrates the impact of pions on observables measured at high-energy facilities such as Fermilab, CERN or DESY, is the $\bar{d} - \bar{u}$ flavour asymmetry of the proton sea. Its first indirect observation came through the violation of the Gottfried sum rule [11], and recently the E866 experiment at Fermilab [12] received considerable attention, as it provided the first detailed mapping of the Bjorken x dependence of the $\bar{d}-\bar{u}$-asymmetry, from a comparison of pp and pd Drell–Yan production. It should be noted, that the strong observed asymmetry has no explanation in terms of purely perturbative QCD dynamics. Thus this effect gives important hints on nonperturbative mechanisms for generating part of the nucleon's sea quark content in addition to the standard perturbative generation of sea quarks from gluon$\to$ $q\bar{q}$ splitting. A natural dynamical explanation of the $\bar{d} - \bar{u}$-asymmetry emerges in the framework of an isovector meson cloud model of the nucleon (for a recent review and references to the early works see [13]). In this picture a special role is played by the pion, and it is intuitively appealing to account for the nonperturbative meson/baryon structure of the proton by including the pion as a nonperturbative parton in the light-cone wavefunction of the interacting nucleon: $|N\rangle_{\rm phys} = |N\rangle_{\rm bare} + |N\pi\rangle + |\Delta\pi\rangle + ...$

Here the pion, which is present in the $N\pi, \Delta\pi$ Fock states, can emerge as a target in the deep inelastic $\gamma^* N$ photoabsorption process, whereas the spectator baryonic constituent, N, Δ, appears in the final state, separated from the products of the $\gamma^*\pi$-interaction by a rapidity gap, and carrying a large fraction z of the initial proton's momentum. Hence inclusive baryon production as in $\gamma^* p \to Xn$ is naturally described in terms of the pionic content of the nucleon. The same dynamics should be at work, if we swap the virtual photon for a proton projectile. This opens the possibility of using a large body of experimental knowledge on inclusive particle production in hadronic reactions to constrain the meson/baryon dynamics relevant for deep inelastic scattering. In the following we shall demonstrate that, if one accounts consistently for the constraints thus derived, a satisfactory description of the Fermilab data emerges [14]. Following the strategy described above, we first turn to the description of forward neutron production in pp collisions. We take three production mechanisms into account: the dominant pion exchange, background contribution from the isovector exchanges ρ and a_2, and finally the production of neutrons from the decay of an intermediate Δ-resonance (see Fig. 4). In addition we have to incor-

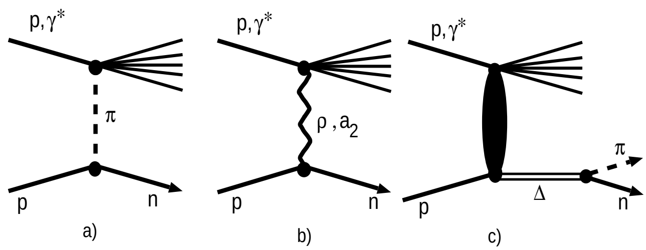

Fig. 4. The mechanisms for inclusive production of forward neutrons. (a) pion exchange, (b) background from (reggeized) ρ, a_2 exchanges, (c) neutrons originating from the decay of an intermediate Δ-resonance.

porate the distortion of the incoming proton waves, employing the standard methods of the generalized eikonal approximation [15]. Following the logic of [15], we apply the absorptive corrections only in pp scattering, they can be neglected in the $\gamma^* p$-case. It is important to note, that the phase space of the forward neutrons includes the kinematical boundary $z \sim 1$, which corresponds to a large Regge parameter $s/M_X^2 \gg 1$, where M_X^2 is the invariant mass squared of the inclusive system X. Hence the proper description of the ρ-exchange mechanism should involve a Regge treatment [16]. We wish to stress that for the pion exchange contribution, Reggeization effects are negligible: due to the proximity of the pion pole, the departure of $\alpha_\pi(t) = \alpha'(t - m_\pi^2)\,, \alpha' \approx 0.7\ \mathrm{GeV}^{-2}$ from $J_\pi = 0$ is small. The finite extension of the particles involved and/or the offshell effects are incorporated in the form factor $F^2_{\pi NN}(t)$. In the figures shown here we use the parametrization $F^2_{\pi NN}(t) = \exp[-(R^2(t - m_\pi^2))^2]\,, R^2 = 1.5\ \mathrm{GeV}^{-2}$. For different choices of the functional form see the discussion in [14]. In Fig. 5 we show our results for the invariant cross section together with the experimental data. The data shown here are at relatively low $p_{\mathrm{LAB}} \approx 24\ \mathrm{GeV}/c$, hence the visible trace of the πN resonance region at large z. The $p_\perp$-dependence nicely illustrates the interplay of the different mechanisms. Pion exchange peaks in the region $0.7 \lesssim z \lesssim 0.9$, and is dominant for $p_\perp \lesssim 0.3\ \mathrm{GeV}$. The relative importance of the ρ, a_2 exchanges grows with $p_\perp$, due to the dominant $\propto p_\perp^2$ spin-flip component of the ρN-coupling. The background contribution from the two-step process $p \to \Delta \to n$ is substantial only for $z \lesssim 0.8$.

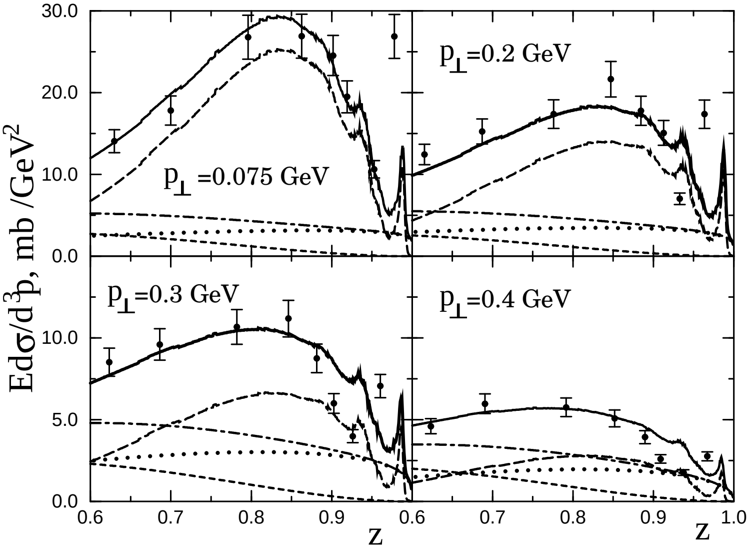

Fig. 5. Invariant cross section for the reaction $pp \to nX$ at $p_{\mathrm{LAB}} = 24\,\mathrm{GeV}/c$. The experimental data are taken from [17]. The long dashed curve shows the contribution of pion exchange; the dotted curve is the ρ, a_2-exchange contribution, and the dashed curve shows the contribution of the two step process $p \to \Delta \to n$. We also show the sum of the two background contributions as the dot-dashed line. Finally, the solid curve is the sum of all contributions.

We have repeatedly stressed the importance of the pion as a nonperturbative parton in the light-cone wavefunction of the interacting proton. There is one more subtle issue related to the Regge form of our production amplitudes, namely what kind of Fock state should be associated with the ρ, a_2 Reggeon exchange production mechanisms, if any? In other words, knowing the reaction mechanisms that populate several inclusive channels, what can we say about their effect on the total cross section? We remind the reader, that one of the firm predictions of Regge theory is a very specific phase for the amplitudes. While the inclusive cross section is calculated from the modulus of the amplitude squared, $|A|^2$, it is the product of two amplitudes, $A \cdot A$, that enters the evaluation of the total cross section. For the purely real pion exchange amplitude, this implies that inelastic interactions of the projectile with the pions in the target hadrons enhance the total cross section, whereas the ρ, a_2-exchanges, which have a phase $\sim (1+i)$, give a vanishing contribution to the total cross section. Thus it is unreasonable to identify the Reggeon exchange mechanism in inclusive reactions with a specific meson/baryon-Fock state of the proton. We note in passing that further constraints on the pion flux can be derived from the inclusive production of forward pions [14].

Following our reasoning above, we include only the πN, $\pi\Delta$- Fock states when calculating the contribution to the proton structure function. In addition to the Fock state parameters determined in our analysis above, we also need as input the quark distributions in the pion. Note, that only the pion's valence distributions enter in the calculation of $\bar{d}(x) - \bar{u}(x)$. These are reasonably well constrained down to $x \sim 0.2$ by Drell–Yan experiments. For definiteness we take the GRV-parametrization [18] . We obtain a total pion multiplicity in the proton due to the πN state of $n_{\pi N} \sim 0.21 \div 0.28$, and $n_{\pi\Delta} \sim 0.03 \ll n_{\pi N}$ for the $\pi\Delta$ contribution. This gives a Gottfried sum of $0.21 \lesssim S_{\mathrm{G}} \lesssim 0.25$, which compares well with the NMC determination [11] $S_{\mathrm{G}} = 0.235 \pm 0.026$. Our result for $\bar{d} - \bar{u}$ is shown in Fig. 6, we observe that the asymmetry is driven essentially by the πN state. Note that our good agreement in the region $x \gtrsim 0.2$ is due to the fact that we have no contributions from hard ($z_\pi \gtrsim 0.5$) pions in the nucleon.

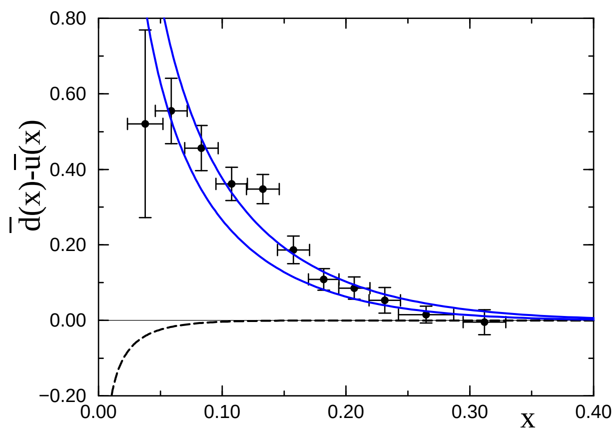

Fig. 6. Flavour asymmetry $\bar{d}(x) - \bar{u}(x)$ at $Q^2 = 54\,\mathrm{GeV}^2$. Experimental data are from E866 [12]. The solid curves show the contribution from the πN Fock state and were calculated assuming Gaussian form factors. The upper curve is for $R_{\mathrm{G}}^2 = 1\,\mathrm{GeV}^{-2}$, and the lower one is $R_{\mathrm{G}}^2 = 1.5\,\mathrm{GeV}^{-2}$. The dashed line shows the contribution of the $\pi\Delta$ Fock state.

Very recent experiments with the forward neutron spectrometer by the ZEUS Collaboration [19] confirm the relevance of the pion exchange to this reaction. The experimental data show all the factorization properties typical of the particle exchange [19], and our model, translated from hadronic production to the deep inelastic case, gives quite reasonable predictions for the measured $p_\perp$ dependence [20].

4. The pion structure function at small x from the colour dipole approach

As we showed above, the study of inclusive forward neutron production allows one to use the nonperturbative pion cloud of the nucleon as a target. Once we fixed the parameters of the πN-Fock state one can now ask the question: What is the total photoabsorption cross section — alias the pion structure function — in an otherwise inaccessible region of small x? Thus the interesting question of the sea quark structure of mesons can be studied experimentally for the first time. Recently the H1 Collaboration [21] has analysed the neutron production data and extracted $F_{2\pi}$, as was proposed by our group in [22]. Interestingly, the behaviour of the pion structure function at small x can be predicted from the colour dipole approach developed in [24]. The crucial observation is that at large values of the Regge parameter $1/x$ the relevant degree of freedom is a colour-dipole, of size and orientation $\boldsymbol{r}$ in the 2-dimensional plane transverse to the γ^*-target collision axis. The colour-dipole states diagonalize the scattering matrix, and the total photoabsorption cross section takes the simple form

$$\sigma^{\gamma^*\pi}(x,Q^2) = \int dz d^2\boldsymbol{r} dz' d^2\boldsymbol{r}' \, |\Psi_{\gamma^*}(z,\boldsymbol{r})|^2 \left|\Psi_\pi(z',\boldsymbol{r}')\right|^2 \cdot \sigma(x,\boldsymbol{r},\boldsymbol{r}') \,. \quad (1)$$

Here $|\Psi_{\gamma^*}(z,\boldsymbol{r})|^2$ is the wavefunction squared for finding a dipole $\boldsymbol{r}$ in the photon with a partition of z and $1-z$ of the photon's lightcone momentum between the quark and antiquark in the colour dipole, *cf.* [24]. $|\Psi_\pi(z',\boldsymbol{r}')|^2$ is the analogous quantity for the pion, which depends only on a size parameter $\langle r_\pi^2\rangle \sim 0.43 fm^2$. The principal dynamical quantity is the dipole–dipole cross section $\sigma(x,\boldsymbol{r},\boldsymbol{r}')$, and the predictive power of the approach derives from the observation, that $\sigma(x,\boldsymbol{r},\boldsymbol{r}')$ can be expanded in a series of isolated Regge poles [23, 24]. This decomposition uniquely prescribes the x-dependence of the dipole–dipole cross section through the solutions of the colour-dipole equation of Nikolaev, Zakharov and Zoller [24], supplemented by an x-independent phenomenological $\sigma_0(r)$ relevant to large, nonperturbative dipole sizes.

All the remaining parameters have been fixed in the phenomenology of the proton structure function (for details see [23]). In Fig. 7 we show the resulting predictions for the pion structure function against the recent data from the H1 Collaboration, and find a good agreement with experiment. It is interesting to note that the result of the calculation follows to a good accuracy the additive quark counting rule $F_{2\pi}(x,Q^2) \simeq \frac{2}{3}F_{2p}\left(\frac{2}{3}x,Q^2\right)$, the dynamical origin of which is quite different for the large, nonperturbative and small, perturbative dipoles (for a discussion see [23]).

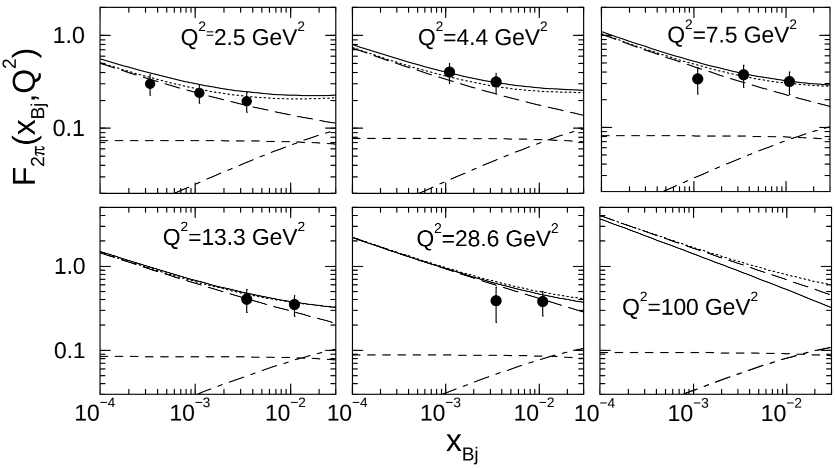

Fig. 7. The pion structure function $F_{2\pi}(x, Q^2)$. The experimental data are from the H1 Collaboration [21]. The solid line shows the colour dipole prediction [23]. The dotted line is the valence contribution, and the dashed line is the contribution from large, nonperturbative dipoles.

5. Summary

We have reviewed the Jülich model for reactions of the type $NN \to NN\pi$. The model is derived in a framework consistent with the interaction potentials that are used to generate amplitudes for the elementary (NN and πN) elastic processes. The NN interaction includes explicit coupling to the $N\Delta$ channel, so that a consistent evaluation of pion production from NN and $N\Delta$ states can be carried out. The πN amplitude is taken from a meson-exchange model of πN scattering developed by the Jülich group. A good overall description of the presently available data for the reaction channels $pp \to pp\pi^0$, $pp \to pn\pi^+$, and $pp \to d\pi^+$ from threshold to the Δ resonance region was achieved. The the inclusion of πN rescattering as well as the Δ degree of freedom played an important role. In the second part we discussed pions in high energy processes. We showed how a consistent phenomenology of inclusive forward neutron production can be used to fix the pionic content of the nucleon, which is relevant for the calculation of the $\bar{d} - \bar{u}$ asymmetry. Good agreement with the recent Drell–Yan data from Fermilab is found. Finally, we compared recent predictions for the small-x behaviour of the pion structure function with experimental data extracted from the forward neutron cross sections.

We would like to thank C. Hanhart, N.N. Nikolaev, A. Szczurek, and V.R. Zoller for collaboration on the topics presented here, and T. Barnes for carefully reading the manuscript. This work was supported in part by the German–Polish exchange grant No. POL-98/028.

REFERENCES

[1] C. Hanhart, J. Haidenbauer, O. Krehl, J. Speth, *Phys. Lett.* **B444**, 25 (1998).

[2] C. Hanhart, J. Haidenbauer, O. Krehl, J. Speth, *Phys. Rev.* **C61**, 064008 (2000).

[3] J. Haidenbauer, K. Holinde, M.B. Johnson, *Phys. Rev.* **C48**, 2190 (1993).

[4] C. Schütz, J.W. Durso, K. Holinde, J. Speth, *Phys. Rev.* **C49**, 2671 (1994).

[5] C. Hanhart, PhD thesis, Jül-3476, Jülich 1998.

[6] H.O. Meyer *et al.*, *Phys. Rev. Lett.* **81**, 3096 (1998).

[7] H.O. Meyer *et al.*, *Phys. Rev. Lett.* **83**, 5939 (1999); P. Thörngren Engblom *et al.*, `nucl-ex/9908024`.

[8] S.K. Saha *et al.*, *Phys. Lett.* **B461**, 175 (1999).

[9] B.V. Przewoski *et al.*, *Phys. Rev.* **C61**, 064604 (2000).

[10] H.O. Meyer, in Baryons '98, Proceedings of the 8th International Conference on the Structure of Baryons, edited by D.W. Menze and B.Ch. Metsch, World Scientific, Singapore 1999, pp. 493.

[11] P. Amaudruz *et al.*, *Phys. Rev. Lett.* **66**, 2712 (1991).

[12] E.A. Hawker *et al.*, *Phys. Rev. Lett.* **80**, 3715 (1998).

[13] J. Speth, A.W. Thomas, *Adv. in Nucl. Phys.* **24**, 84 (1998).

[14] N.N. Nikolaev, W. Schäfer, J. Speth, A. Szczurek, *Phys. Rev.* **D60**, 014004 (1999).

[15] N.N. Nikolaev, J. Speth, B.G. Zakharov, `hep-ph/9708290`.

[16] A. Szczurek, N.N. Nikolaev, J. Speth, *Phys. Lett.* **B428**, 383 (1998).

[17] V. Blobel *et al.*, *Nucl. Phys.* **B135**, 379 (1978).

[18] M. Glück, E. Reya, A. Vogt, *Z. Phys.* **C53**, 651 (1992).

[19] W. Schmidke for H1 and ZEUS Collab., Talk at the 8th Int. Workshop on deep inelastic scattering and QCD, DIS2000, Liverpool, April 2000.

[20] W. Schäfer, N. Nikolaev, J. Speth, A. Szczurek, *Acta Phys. Pol.* **B31**, 2511 (2000).

[21] H1 Collab., C. Adloff *et al.*, *Eur. Phys. J.* **C6**, 587 (1999).

[22] H. Holtmann *et al.*, *Phys. Lett.* **B338**, 363 (1994).

[23] N.N. Nikolaev, J. Speth, V.R. Zoller, *Phys. Lett.* **B473**, 157 (2000).

[24] see N.N. Nikolaev *et al.*, *JETP Lett.* **66**, 138 (1997) and references therein.